View metadata, citation and similar papers at core.ac.uk

brought to you by CORE

provided by Michigan Technological University

Michigan Technological University

Digital Commons @ Michigan Tech

Michigan Tech Publications

1-1-2020

Micromechanical Prediction Model of Viscoelastic Properties for Asphalt Mastic Based on Morphologically Representative Pattern Approach

Zhichen Wang
Dalian Maritime University

Naisheng Guo
Dalian Maritime University

Xu Yang
Michigan Technological University, xyang2@mtu.edu

Shuang Wang
Lyceum of the Philippines University

Follow this and additional works at: https://digitalcommons.mtu.edu/michigantech-p

Recommended Citation

Wang, Z., Guo, N., Yang, X., & Wang, S. (2020). Micromechanical Prediction Model of Viscoelastic Properties for Asphalt Mastic Based on Morphologically Representative Pattern Approach. *Advances in Materials Science and Engineering, 2020*. http://doi.org/10.1155/2020/7915140
Retrieved from: https://digitalcommons.mtu.edu/michigantech-p/2758

Follow this and additional works at: https://digitalcommons.mtu.edu/michigantech-p

Hindawi
Advances in Materials Science and Engineering
Volume 2020, Article ID 7915140, 12 pages
https://doi.org/10.1155/2020/7915140

Research Article

Micromechanical Prediction Model of Viscoelastic Properties for Asphalt Mastic Based on Morphologically Representative Pattern Approach

Zhichen Wang,[1] Naisheng Guo ,[1] Xu Yang ,[2] and Shuang Wang[3]

[1]*School of Transportation Engineering, Dalian Maritime University, Dalian 116026, Liaoning, China*
[2]*Department of Civil and Environmental Engineering, Michigan Technological University, Houghton, MI 49931-1295, USA*
[3]*School of Computer Science, Lyceum of the Philippines University, Manila, Batangas 4200, Philippines*

Correspondence should be addressed to Naisheng Guo; naishengguo@dlmu.edu.cn

Received 16 April 2020; Accepted 3 June 2020; Published 28 June 2020

Guest Editor: Meng Guo

Copyright © 2020 Zhichen Wang et al. This is an open access article distributed under the Creative Commons Attribution License, which permits unrestricted use, distribution, and reproduction in any medium, provided the original work is properly cited.

This paper is devoted to the introduction of physicochemical, filler size, and distribution effect in micromechanical predictions of the overall viscoelastic properties of asphalt mastic. In order to account for the three effects, the morphologically representative pattern (MRP) approach was employed. The MRP model was improved due to the arduous practical use of equivalent modulus formula solution. Then, a homogeneous morphologically representative model (H-MRP) with the explicit solution was established based on the homogenization theory. Asphalt mastic is regarded as a composite material consisting of filler particles coated structural asphalt and free asphalt considering the physicochemical effect. An additional interphase surrounding particles was introduced in the H-MRP model. Thus, a modified H-MRP model was established. Using the proposed model, a viscoelastic equation was derived to predict the complex modulus and subsequently the dynamic modulus of asphalt mastic based on the elastic-viscoelastic correspondence principle. The dynamic shear rheological tests were conducted to verify the prediction model. The results show that the predicted modulus presents an acceptable precision for asphalt mastic mixed with 10% and 20% fillers volume fraction, as compared to the measured ones. The predicted modulus agrees reasonably well with the measured ones at high frequencies for asphalt mastic mixed with 30% and 40% fillers volume fraction. However, it exhibits underestimated modulus at low frequencies. The reasons for the discrepancy between predicted and measured dynamic shear modulus and the factors affecting the dynamic shear modulus were also explored in the paper.

1. Introduction

Asphaltic material is a typical rheological material. Asphalt mastic is regarded as a composite material consisting of asphalt and fillers, which plays an essential role in the binding between aggregates in asphalt mixture. Dynamic shear modulus is the leading indicator to evaluate the viscoelastic properties of asphalt mastic. A large number of dynamic shear rheological tests have been conducted to explore the influence of different asphalt and fillers on the dynamic shear modulus of asphalt mastic [1–3]. However, plenty of factors are influencing the viscoelastic properties of asphalt mastic, and it is unrealistic and uneconomic to analyze these factors through a large amount of tests. Thus, it is necessary to propose the prediction methods that can be used to obtain the dynamic shear modulus of asphalt mastic.

The empirical prediction models were proposed under the support of NCHRP, including the Witczak 1–37A model, improved Witczak model, and NCHRP 1–40D model [4–6]. In order to provide the parameters of asphalt binder for the prediction model of asphalt mixtures, an empirical prediction model for the dynamic shear modulus of asphalt binder was established by Bari and Witczak [7]. However, the model was adopted under specific conditions in the United States, and it may not be applicable in other regions. Therefore, it is necessary to get rid of the empirical method and predict the macroscopic properties from the volume and mechanical properties of the components. The

micromechanics method of composite materials provides a reliable method for this work.

The classical micromechanical methods of composite materials, including composite sphere model [8], self-consistent model [9], generalized self-consistent model (Christensen Lo model) [10], and Mori Tanaka method [11], have been widely used in the equivalent properties prediction of the particle and fiber-reinforced composite materials. Some scholars applied these classical micromechanical methods to establish the micromechanical model of asphalt mixtures. Pang et al. utilized a composite sphere model to predict the elastic modulus of the asphalt mixture [12]. Luo et al. adopted the self-consistent model and generalized self-consistent model to predict the dynamic modulus of the asphalt mixture [13, 14]. Zhu et al. presented a micromechanical model considering the effect of the interface between asphalt and aggregate [15, 16].

Asphalt mastic was considered as a known matrix in the above prediction models. The modulus test of asphalt mastic should be conducted repeatedly to provide the input parameters for the models due to the variety of the fillers concentration. Therefore, it is also necessary to establish the micromechanical model of asphalt mastic. Asphalt mastic is regarded as a composite material composed of spherical filler particles embedded in asphalt binder. A lot of different methods have been presented to establish the micromechanical model of asphalt mastic. Yin et al. applied four micromechanics methods, that is, dilution model, self-consistent model, generalized self-consistent model, and Mori Tanaka method, to predict the dynamic shear modulus of asphalt mastic [17]. Underwood and Kim presented 12 existing micromechanical methods to predict the dynamic shear modulus of asphalt mastic [18]. However, the results show that the micromechanical model considerably underestimates the viscoelastic properties of asphalt mastic.

The percolation effect of fillers and asphalt is considered by Shashidhar and Shenoy [19]. There is an increasing probability of the particles touching one another and the filler becoming percolated; then a modified method was proposed for the prediction model by percolation theory. They use the calculation to suggest that percolation phenomenon onset occurs at 2%–10%. However, the mechanical data compiled by multiple scholars suggest that a filler concentration of approximately 42% is more appropriate for asphalt mastics [20–22]. Li et al. utilized Ju-Chen model to predict the dynamic shear modulus of asphalt mastic considering the interparticle interaction [23]. However, the interaction between fillers is difficult to measure, and it is not easy to judge whether it actually occurred. Therefore, it is necessary to ascertain the interior structural components and interaction mechanism of asphalt mastic and to establish a targeted micromechanical model.

An experiment was conducted by Davis and Castorena using atomic force microscopy [24]. The microscopic variation of asphalt near the filler particle surface was founded, which indicated that the physicochemical effect has occurred between the fillers and asphalt. The physicochemical process of selective adsorption of the asphalt binder compounds by the aggregate particles occurring in asphaltic composites is also widely reported [25–27]. A structural asphalt layer will be formed on the surface of the fillers under the physicochemical effect; thus, a four-phase micromechanical model of asphalt mastic was proposed by Underwood and Kim [18]. The model is based on the classical n-layer sphere model derived from point-approaches, according to which the Representative Volume Element (RVE) is defined through some statistical information on points belonging to such or such phase. It is meaningless to endow them with any individual geometrical or physical specific property of these phase elements, such as their size, their mutual distances, or their superficial area. Thus, the influence of the particle size and distribution of fillers were not taken into consideration in the four-phase micromechanical model.

In order to consider the distribution and size effects in micromechanical predictions model, a morphologically representative pattern (MRP) approach has been proposed for composite materials [28, 29], which could be applied for asphalt mastic. The objective of this paper strives to establish a new micromechanical model considering the physicochemical, filler size, and distribution effect based on the MRP approach. The new proposed model is used to predict the dynamic shear modulus of asphalt mastic, and the prediction results were compared with the experiment results of the asphalt mastic with different filler volume fractions to validate its applicability. In additions, the influence of model parameters on the prediction results is also analyzed.

2. Micromechanical H-MRP Model

Marcadon et al. proposed a morphology representative pattern (MRP) model considering distribution and size effects in micromechanical predictions of the overall elastic moduli of particulate composite materials [28]. The composition of MRP model comes from the composite sphere model [8]. However, the spherical particles with different particle sizes are replaced by a series of spherical particles with the same particle size. The MRP model consists of matrix-coated spheres (two-phase pattern) and the remaining matrix (pure matrix pattern); see Figure 1.

The far-field uniform strain of two patterns is equal to the total strain, $\langle \varepsilon \rangle = \mathbf{E}$. Marcadon et al. obtained the equivalent modulus solution formula of the MRP model characterized by nonlinear equations [28]. Although mathematical software such as Mathematica can be used for auxiliary calculation, some negative solutions appear frequently, which make it difficult to be applied. The homogenization method is employed to improve the MRP model. The two-phase pattern in the MRP model is homogenized into an equivalent medium by using the generalized self-consistent method. Subsequently, the medium is put into the remaining matrix. The self-consistent method is applied for homogenization into the equivalent composite material. Thus, an improved model is established, called homogenized MRP model (H-MRP), as shown in Figure 2.

According to the MRP approach, each pattern consists of one particle surrounded by a concentric shell of the matrix of variable thickness depending on the packing density, with an

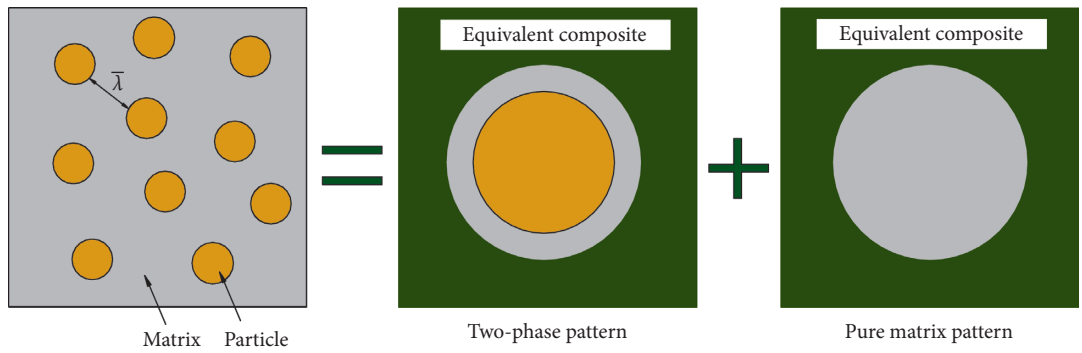

Figure 1: MRP model.

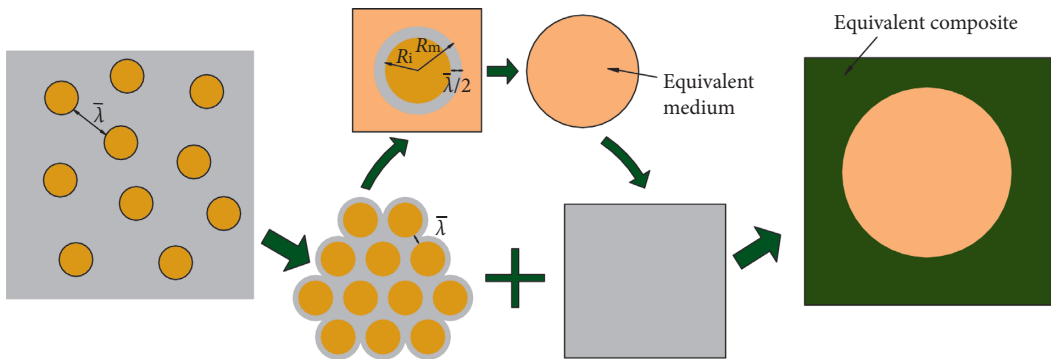

Figure 2: Homogenized MRP model (H-MRP model).

additional pattern of the residual pure matrix. The shell thickness may then be correlated with the mean distance between nearest-neighbor particles, say $\overline{\lambda}$. The first two patterns are made of two concentric spheres, with a particle at the core and a shell, with the thickness $R_m - R_i = (\overline{\lambda}/2)$, constituted with the pure matrix. Therefore, the volume fraction of particles in the two-pattern approach c_i is calculated as

$$c_i = \frac{f_i}{c_H} = \frac{R_i^3}{R_m^3} = \frac{R_i^3}{\left(R_i + (\overline{\lambda}/2)\right)^3} = \frac{1}{\left(1 + \left(\overline{\lambda}/(2R_i)^3\right)\right)}, \quad (1)$$

where f_i is the volume fraction of inclusions; c_H is the volume fraction of two-phase pattern; R_i and R_m are the particle and matrix radius, respectively. From equation (1), it is apparent already that the effective properties simultaneously depend on the particle size R_i and on the mean distance $\overline{\lambda}$ through the ratios $(\overline{\lambda}/(2R_i))$, so that $(\overline{\lambda}/(2R_i))$ is defined as the particle distribution coefficient. It is an important parameter reflecting particle distribution characteristics.

According to the composite sphere (CS) model [8], the bulk modulus of the equivalent medium K_H can be obtained by

$$K_H = K_m + \frac{c_i(K_i - K_m)(3K_m + 4G_m)}{3K_m + 4G_m + 3(1 - c_i)(K_i - K_m)}, \quad (2)$$

where K_i and K_m are the bulk moduli of inclusions and matrix, respectively; G_m is the shear modulus of the matrix.

According to the generalized self-consistent (GSC) model [10], the shear modulus of the equivalent medium G_H is given by

$$A\left(\frac{G_H}{G_m}\right)^2 + 2B\left(\frac{G_H}{G_m}\right) + C = 0, \quad (3)$$

where A, B, and C are functions related to the modulus and volume fraction of particles and matrix, expressed as

$$A = 8\left(\frac{G_i}{G_m} - 1\right)(4 - 5\nu_m)\eta_1 c_i^{10/3} - 2\left[63\left(\frac{G_i}{G_m} - 1\right)\eta_2 + 2\eta_1\eta_3\right]c_i^{7/3} + 252\left(\frac{G_i}{G_m} - 1\right)\eta_2 c_i^{5/3} - 50\left(\frac{G_i}{G_m} - 1\right)\left(7 - 12\nu_m + 8\nu_m^2\right)\eta_2 c_i + 4(7 - 10\nu_m)\eta_2\eta_3, \quad (4)$$

$$B = -2\left(\frac{G_i}{G_m} - 1\right)(1 - 5\nu_m)\eta_1 c_i^{10/3} + 2\left[63\left(\frac{G_i}{G_m} - 1\right)\eta_2 + 2\eta_1\eta_3\right]c_i^{7/3} - 252\left(\frac{G_i}{G_m} - 1\right)\eta_2 c_i^{5/3} + 75\left(\frac{G_i}{G_m} - 1\right)(3 - \nu_m)\eta_2\nu_m c_i + \frac{3}{2}(15\nu_m - 7)\eta_2\eta_3, \quad (5)$$

$$C = 4\left(\frac{G_i}{G_m} - 1\right)(5\nu_m - 7)\eta_1 c_i^{10/3} - 2\left[63\left(\frac{G_i}{G_m} - 1\right)\eta_2 + 2\eta_1\eta_3\right]c_i^{7/3} + 252\left(\frac{G_i}{G_m} - 1\right)\eta_2 c_i^{5/3} + 25\left(\frac{G_i}{G_m} - 1\right)\left(\nu_m^2 - 7\right)\eta_2 c_i - (7 + 5\nu_m)\eta_2\eta_3, \tag{6}$$

$$\eta_1 = (49 - 50\nu_i\nu_m)\left(\frac{G_i}{G_m} - 1\right) + 35\left[\frac{G_i}{G_m}(\nu_i - 2\nu_m) + (2\nu_i - \nu_m)\right], \tag{7}$$

$$\eta_2 = 5\nu_i\left(\frac{G_i}{G_m} - 8\right) + 7\left(\frac{G_i}{G_m} + 4\right), \tag{8}$$

$$\eta_3 = \frac{G_i}{G_m}(8 - 10\nu_m) + (7 - 5\nu_m), \tag{9}$$

where ν_m is Poisson's ratio of the matrix.

The equivalent shear modulus can be written in an explicit expression as

$$G_H = \frac{\sqrt{B^2 - AC} - B}{A}G_m. \tag{10}$$

The equivalent medium is embedded in the remaining matrix. From equation (1), the volume fraction of equivalent medium c_H is given by

$$c_H = \frac{f_i}{c_i} = f_i\left(1 + \frac{\overline{\lambda}}{2R_i}\right)^3. \tag{11}$$

According to the self-consistent (SC) model [9], the bulk modulus K_c and shear modulus G_c of the composite can be obtained as follows:

$$K_c = K_m + \frac{c_H(K_H - K_m)(3K_c + 4G_c)}{3K_H + 4G_c}, \tag{12}$$

$$G_c = G_m + \frac{5c_H G_c(G_H - G_m)(3K_c + 4G_c)}{3K_c(3G_c + 2G_H) + 4G_c(2G_c + 3G_H)}. \tag{13}$$

It can be found that the explicit expressions of the GSC model and SC model are used to obtain the equivalent modulus of the composite, which is convenient for engineering application.

The spherical particles and the matrix in the composite are regarded as elastic materials. Let Young's modulus ratio $(E_i/E_m) = 10$ and Poisson's ratio $\nu_i = \nu_m = 0.3$; the MRP model was employed to predict the equivalent modulus of composite with different particle distribution coefficient by Majewski et al. [29]. The predicted results of H-MRP model are obtained by using the same model parameters as the MRP model. The comparison results are shown in Figures 3(a) and 3(b).

It can be seen from Figure 3 that the prediction results of H-MRP model proposed in this study are consistent with the MRP model. The predicted modulus of the H-MRP model is between the GSC model and SC model. Since the predicted results of the H-MRP model are related to the mean minimum distance between nearest-neighbor particles $\overline{\lambda}$, there are two limit cases: (1) When $\overline{\lambda} = 0$, the thickness of the particle-coated matrix layer in the composite sphere is 0. The equivalent material is still spherical particles after homogenization, which is equivalent to the self-consistent model. Therefore, the upper limit of the H-MRP model is the SC model. (2) When the particles in the composite sphere coated the overall matrix, there is no remaining matrix, expressed as

$$\frac{\overline{\lambda}}{(2R_i)} = f_i^{-(1/3)} - 1. \tag{14}$$

It is equivalent to the GSC model, so the lower limit of the H-MRP model is the GSC model.

3. Micromechanical Model of Asphalt Mastic considering the Physicochemical Effect

A structural asphalt layer on the surface of fillers should be produced by physicochemical interaction between asphalt and fillers, and the outside of it is a free asphalt layer without physicochemical effect. Therefore, it is proposed to transform the two-phase pattern of spherical filler particles coated asphalt in H-MRP model into a three-phase pattern of fillers coated structural and free asphalt. The modified H-MRP model is shown in Figure 4.

When studying distribution effects in Section 2, we already noticed (see Figure 2) that a GSC model and SC model are chosen. A similar conclusion can be drawn with the 4-phase model [30] when coated particles are dealt with (see Figure 4). Let R_1, R_2, and R_3 be, respectively, the radii of the three different spheres in the composite sphere in Figure 4, by beginning the numbering from the center of the composite sphere.

The effective moduli K_{eff} and G_{eff} of the equivalent medium are then determined from equations (46) and (51) of Herve and Zaoui [30].

$$K_{\text{eff}} = K_3 + \frac{(3K_3 + 4G_3)R_2^3[(K_1 - K_2)R_1^3(3K_3 + 4G_2) + (K_2 - K_3)R_2^3(3K_1 + 4G_2)]}{3(K_2 - K_1)R_1^3[R_2^3(3K_3 + 4G_2) + 4R_3^3(G_3 - G_2)] + (3K_1 + 4G_2)R_2^3[3R_2^3(K_3 - K_2) + R_3^3(3K_3 + 4G_3)]}, \tag{15}$$

$$G_{\text{eff}} = \frac{\sqrt{B'^2 - A'C'} - B'}{A'}G_3, \tag{16}$$

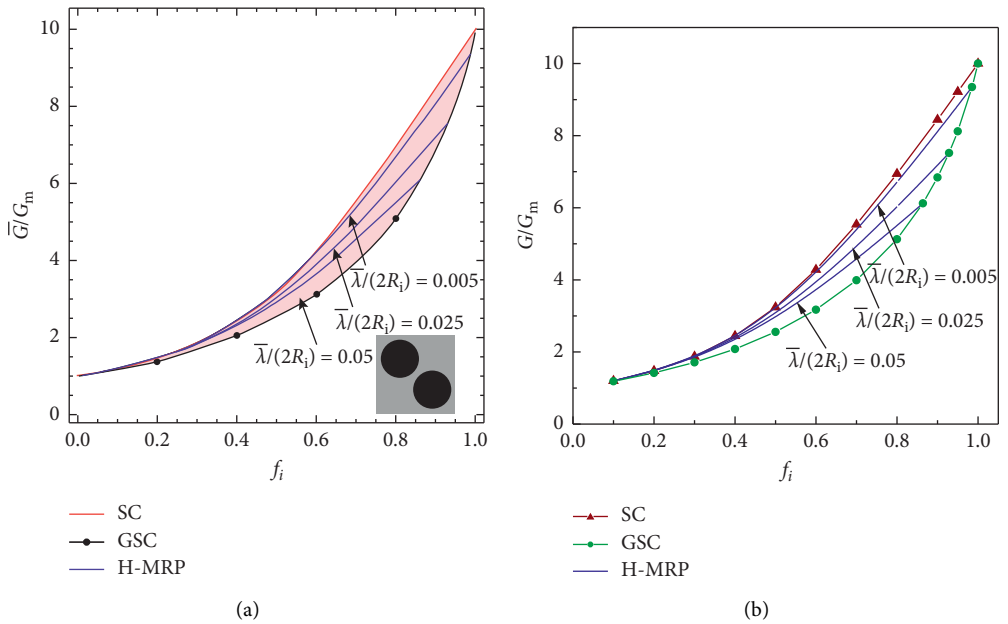

Figure 3: Predicted results of the micromechanical model under different particle distribution coefficients. (a) MRP model [29]. (b) H-MRP model

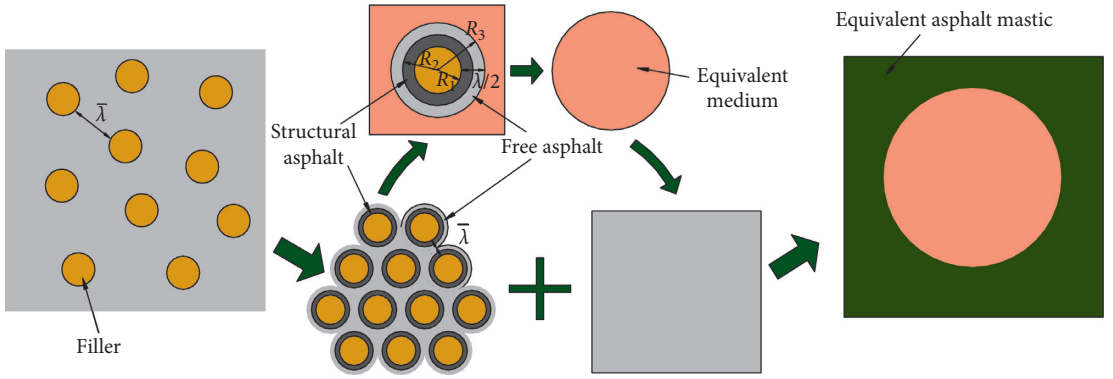

Figure 4: Modified H-MRP model.

where R_1, R_2, and R_3 are the radii of fillers, structural asphalt, and free asphalt, respectively. A', B', and C' are given by

$$A' = 4R_3^{10}(1-2\nu_3)(7-10\nu_3)Z_{12} + 20R_3^7\left(7-12\nu_3+8\nu_3^2\right)Z_{42} + 12R_3^5(1-2\nu_3)(Z_{14}-7Z_{23}) + 20R_3^3(1-2\nu_3)^2Z_{13} + 16(4-5\nu_3)(1-2\nu_3)Z_{43}, \tag{17}$$

$$B' = 3R_3^{10}(1-2\nu_3)(15\nu_3-7)Z_{12} + 60R_3^7(\nu_3-3)\nu_3Z_{42} - 24R_3^5(1-2\nu_3)(Z_{14}-7Z_{23}) - 40R_3^3(1-2\nu_3)^2Z_{13} - 8(1-5\nu_3)(1-2\nu_3)Z_{43}, \tag{18}$$

$$C' = -R_3^{10}(1-2\nu_3)(7+5\nu_3)Z_{12} + 10R_3^7\left(7-\nu_3^2\right)\nu_3Z_{42} + 12R_3^5(1-2\nu_3)(Z_{14}-7Z_{23}) + 20R_3^3(1-2\nu_3)^2Z_{13} - 8(7-5\nu_3)(1-2\nu_3)Z_{43}, \tag{19}$$

$$Z_{\alpha\beta} = \widetilde{P}_{\alpha1}^{(2)}\widetilde{P}_{\beta2}^{(2)} - \widetilde{P}_{\beta1}^{(2)}\widetilde{P}_{\alpha2}^{(2)}, \tag{20}$$

$$\mathbf{P}^{(n)} = \prod_{k=1}^{3}\mathrm{M}^{(k)}, \tag{21}$$

$$\mathrm{M}^{(k)} = \mathbf{L}_{k+1}^{-1}(R_k)\mathbf{L}_k(R_k), \tag{22}$$

with

$$\mathbf{L}_k(r) = \begin{bmatrix} r & -\frac{6\nu_k}{1-2\nu_k}r^3 & \frac{3}{r^4} & \frac{5-4\nu_k}{1-2\nu_k}\frac{1}{r^2} \\ r & -\frac{7-4\nu_k}{1-2\nu_k}r^3 & -\frac{2}{r^4} & \frac{2}{r^2} \\ G_k & \frac{3\nu_k}{1-2\nu_k}G_k r^2 & -\frac{12}{r^5}G_k & \frac{2(\nu_i-5)}{1-2\nu_k}\frac{G_k}{r^3} \\ G_k & -\frac{7+2\nu_k}{1-2\nu_k}G_k r^2 & \frac{8}{r^5}G_k & \frac{2(1+\nu_k)}{1-2\nu_k}\frac{G_k}{r^3} \end{bmatrix}. \quad (23)$$

The viscoelastic properties of the equivalent medium can be directly converted from the elastic solutions from the micromechanical models using the elastic-viscoelastic correspondence principle. The correspondence principle states that the effective complex material properties for a viscoelastic material can be obtained by replacing the elastic material properties by the Laplace transformed material properties [31, 32]. It is reasonable to assume that structural asphalt and free asphalt are viscoelastic, while fillers are elastic. Based on the elastic-viscoelastic correspondence principle, equations (15) and (16) can be expressed in the frequency domain as follows:

$$K_{\text{eff}}^* = K_3^* + \frac{(3K_3^*+4G_3^*)R_2^3\left[(K_1-K_2^*)R_1^3(3K_3^*+4G_2^*)+(K_2^*-K_3^*)R_2^3(3K_1+4G_2^*)\right]}{3(K_2^*-K_1)R_1^3\left[R_2^3(3K_3^*+4G_2^*)+4R_3^3(G_3^*-G_2^*)\right]+(3K_1+4G_2^*)R_2^3\left[3R_2^3(K_3^*-K_2^*)+R_3^3(3K_3^*+4G_3^*)\right]}, \quad (24)$$

$$G_{\text{eff}}^* = \frac{\sqrt{B''^2-A''C''}-B''}{A''}G_3^*, \quad (25)$$

where K_{eff}^* and G_{eff}^* are the complex moduli of the equivalent medium. K_2^*, G_2^*, K_3^*, and G_3^* are the complex moduli of the structural asphalt and free asphalt, respectively. A'', B'', and C'' are derived from equations (17) to (23) by replacing G_k by ${G_k}^*$ and ν_k by ${\nu_k}^*$.

From equations (12) and (13), the complex bulk modulus K_{ms}^* and complex shear modulus G_{ms}^* of asphalt mastic are given by

$$K_{\text{ms}}^* = K_3^* + \frac{c_{\text{eff}}(K_{\text{eff}}^*-K_3^*)(3K_{\text{ms}}^*+4G_{\text{ms}}^*)}{3K_{\text{eff}}^*+4G_{\text{ms}}^*}, \quad (26)$$

$$G_{\text{ms}}^* = G_3^* + \frac{5c_{\text{eff}}G_{\text{ms}}^*(G_{\text{eff}}^*-G_3^*)(3K_{\text{ms}}^*+4G_{\text{ms}}^*)}{3K_{\text{ms}}^*(3G_{\text{ms}}^*+2G_{\text{eff}}^*)+4G_{\text{ms}}^*(2G_{\text{ms}}^*+3G_{\text{eff}}^*)}, \quad (27)$$

where c_{eff} is the volume fraction of equivalent medium, calculated as

$$c_{\text{eff}} = \frac{f_1}{c_1} = f_1 1 + \left(\frac{\overline{\lambda}}{(2R_1)^3}\right), \quad (28)$$

where f_1 is the volume fraction of fillers in asphalt mastic; c_1 is the volume fraction of fillers in three-phase pattern.

The storage modulus G' and loss modulus G'' of asphalt mastic are calculated from equations (26) and (27) by using the complex modulus relation $G^* = G' + iG''$. The dynamic shear modulus of asphalt mastic $|G^*|$ is calculated as

$$|G^*| = \sqrt{(G')^2+(G'')^2}. \quad (29)$$

4. Viscoelastic Properties Prediction and Validation for Asphalt Mastic

The dynamic shear modulus of asphalt mastic with different filler volume fractions was collected from the literature reported by Underwood and Kim [18]. The volume fractions of fillers are, respectively, 10% (MS10), 20% (MS20), 30% (MS30), and 40% (MS40). Based on the time-temperature equivalence principle, the master curves of the dynamic shear modulus of asphalt mastic $|G_{\text{ms}}^*|$ are shown in Figure 5.

The fillers in asphalt mastic are stone materials, and the elastic modulus and Poisson's ratio of the filler could be valued as $E_1 = 56$ GPa and $\nu_1 = 0.25$ [32]. Di Benedetto obtained that Poisson's ratio of the asphalt varies with frequency from 0.48 to 0.5, and the phase angle is from −0.18 to −1.29° [33]. Approximate values of 0.49 and 0° are used as Poisson' s ratio and phase angle of asphalt for computing convenience.

Assuming that the fillers are uniformly distributed as body-centered cubic, the fillers distribution coefficient is shown as [29]

$$\frac{\overline{\lambda}}{(2R_1)} = \left[\frac{\sqrt{3}\,\pi}{(8f_1)}\right]^{1/3} - 1. \quad (30)$$

The fillers are regarded as spherical; the cumulative passing percentage of particle size d_i of the fillers is expressed as P_i, $(i = 1, \ldots, m)$. The average particle size of sieve i is represented by $(d_i + d_{i-1})/4$. The number of filler particles of sieve i in unit mass N_i is expressed as

$$N_i = \frac{(P_i - P_{i-1})}{\rho_{\text{f}}(4/3)\pi\left((d_i+d_{i-1})/4\right)^3}, \quad (31)$$

where ρ_{f} is the density of fillers.

From equation (31), the specific surface area of filler particles S_{f} is given by

$$S_{\text{f}} = \sum_{i=1}^{m} 4\pi\left(\frac{d_i+d_{i-1}}{4}\right)^2 N_i. \quad (32)$$

The number of filler particles in asphalt mastic is N; the relationship between the average radius $\overline{R}$ of all spherical particles and the specific surface area S is calculated as

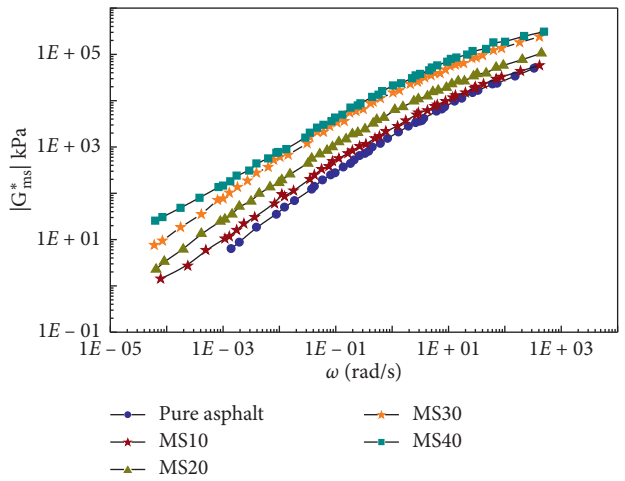

Figure 5: Master curves of the dynamic shear modulus of asphalt mastic.

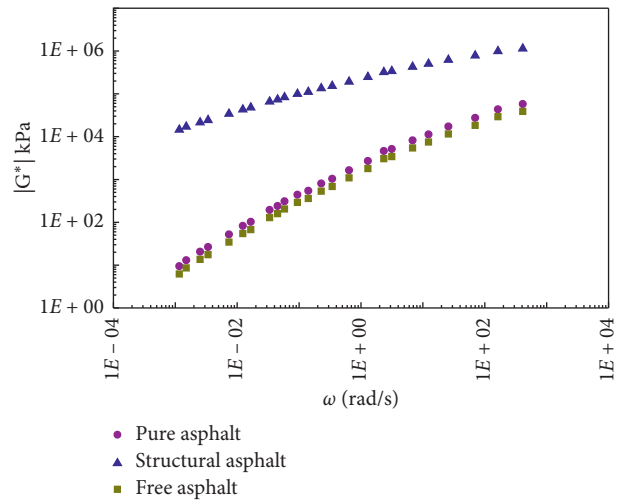

Figure 6: Dynamic shear modulus of structural asphalt and free asphalt.

$$S = \frac{4\pi \overline{R}^2 N}{(4/3)\pi \overline{R}^3 \rho_f N} = \frac{3}{\overline{R}\rho_f}. \tag{33}$$

From equation (33), the average radius of filler particles is given by

$$\overline{R} = \frac{3}{S\rho_f}. \tag{34}$$

The dynamic shear moduli of structural asphalt in equations (24) and (25) are assumed to satisfy the logarithmic mean value relationship between filler and asphalt. The complex shear modulus of structural asphalt can be expressed as

$$G_2^* = 10^{\left((\lg G_1 + \lg G_{ba}^*)/2\right)}, \tag{35}$$

where G_1 and G_{ba}^* are the complex shear moduli of fillers and asphalt, respectively.

The mixed model proposed by Underwood and Kim [18] is employed to characterize the interaction between structural asphalt and free asphalt; the complex shear modulus of free asphalt can be obtained:

$$\left|G_3^*\right| = \frac{\left|G_{ba}^*\right| \times \left|G_2^*\right| \times c_3}{\left|G_2^*\right| - \left|G_{ba}^*\right| \times c_2}, \tag{36}$$

where c_2 and c_3 are the volume fractions of structural asphalt and free asphalt in the total asphalt.

Figure 6 shows the dynamic shear moduli of structural asphalt and free asphalt calculated from equations (35) and (36). It can be seen that the structural asphalt absorbs the polar component of the matrix asphalt until it is saturated, which leads to a significant increase in the complex modulus. A small number of polar components are lost in the free asphalt, resulting in a slight decrease in the complex modulus.

The thickness of the structural asphalt layer is related to the physicochemical reaction between asphalt and fillers. Underwood et al. have obtained that the thickness of structural asphalt layer is 0.2–0.63 μm when the volume fraction of fillers in asphalt mastic is 10%–60% by microscopic analysis. Therefore, the volume fraction of structural asphalt was determined as $c_{sa} = 30\%$, and the structural asphalt thickness d_s and volume fraction of each component are calculated as shown in Table 1.

The H-MRP and modified H-MRP models are applied to predict the dynamic shear modulus of asphalt mastic $|G_{ms}^*|$ with different filler volume fractions. Figure 7 presents the predicted and measured $|G_{ms}^*|$ values for asphalt mastic. It can be seen that when the volume fraction of fillers is 10% and 20%, the predicted results of the two models are close to the measured ones. However, the predicted modulus of the modified H-MRP model is higher than the measured modulus at high frequency. It shows that when the content of fillers is low, the physicochemical effect between asphalt and fillers may be weak. Therefore, the volume fraction of structural asphalt assumed as $c_{sa} = 30\%$ overestimates the physicochemical effects. The volume fraction of structural asphalt should be lower than 30%; however, when the volume fraction of structural asphalt is 0%, the modified H-MRP model is equivalent to the H-MRP model. It can be seen from Figures 7(a) and 7(b) that the modulus predicted by the H-MRP model is closer to the measured modulus than the modified H-MRP model. Therefore, it is suggested to apply H-MRP model to predict the viscoelasticity of asphalt mastic, while the volume fraction is less than 20%.

When the volume fractions of fillers are 30% and 40%, the predicted value of the modified H-MRP model is closer to the measured ones compared with the H-MRP model, which could be attributed to the fact that the physicochemical effect is strengthened when the volume fractions of fillers are high, so it is reasonable to assume $c_{sa} = 30\%$. The predicted dynamic modulus is much closer to the measured ones at high frequencies than at low frequencies. It indicated that the proposed models underestimated the viscoelastic effect of asphalt at low frequencies, asphalt mastic can be considered as asphalt with the addition of fillers in it, and fillers are basically elastic. With the elastic fillers added to asphalt, the proportions of the elastic and viscous

Table 1: Thickness of structural asphalt layer and volume fraction of each component.

Mastic types	d_s (μm)	Asphalt mastic			Asphalt	
		Fillers (%)	Structural asphalt (%)	Free asphalt (%)	Structural asphalt (%)	Free asphalt (%)
MS10	2.22	10	27.1	62.9	30.1	69.9
MS20	1.22	20	24.1	55.9	30.1	69.9
MS30	0.79	30	21.2	48.8	30.2	69.8
MS40	0.54	40	18.2	41.8	30.3	69.7

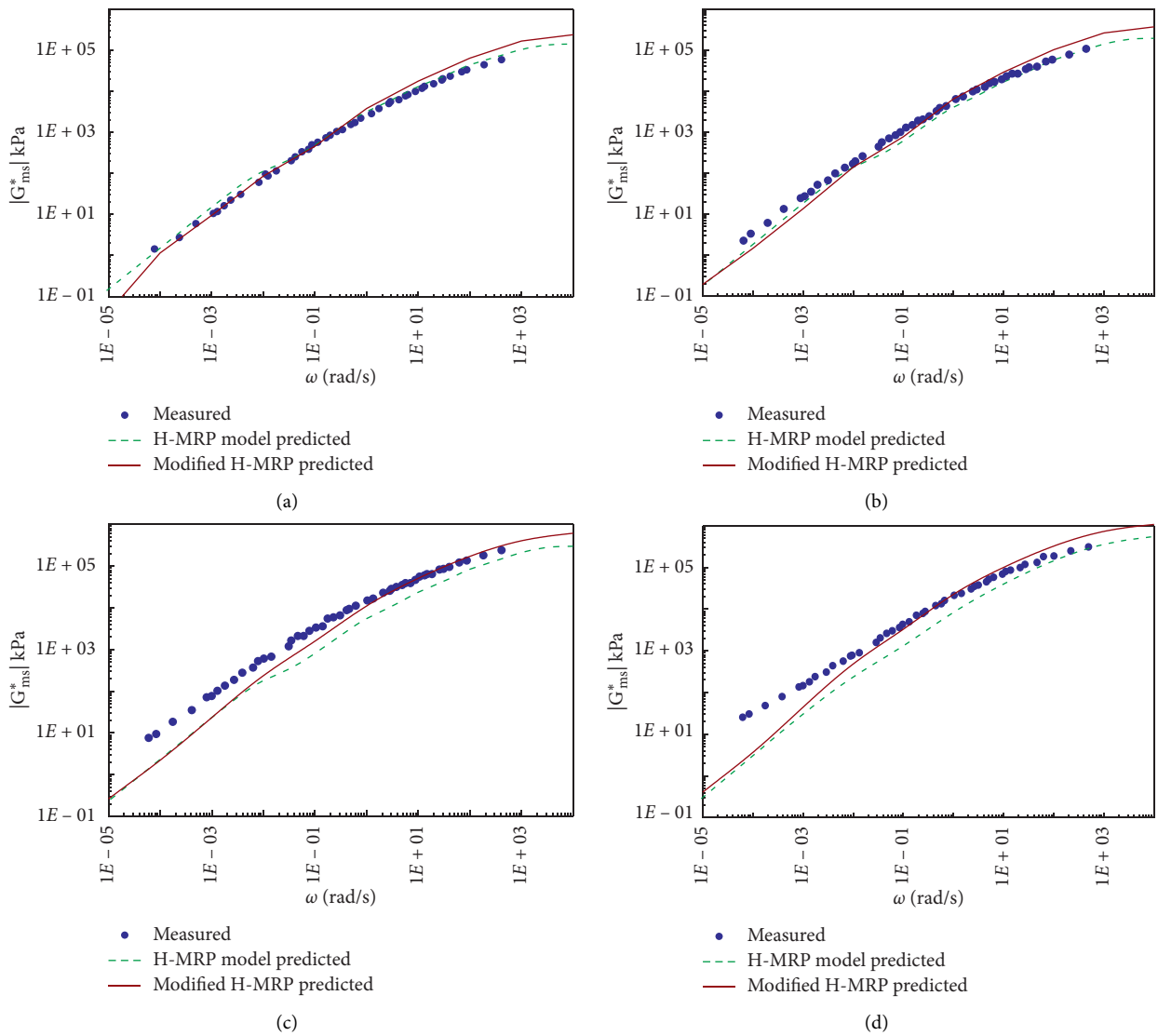

Figure 7: Comparison of predicted and measured $|G^*_{ms}|$ values. (a) MS10. (b) MS20. (c) MS30. (d) MS40.

components in asphalt mastic are different from those in pure asphalt, which will definitely cause the change in the elastic and viscous components of the complex modulus. Therefore, asphalt mastic should exhibit higher modulus than that of pure asphalt due to the addition of elastic fillers. The dynamic modulus is not a linear elasticity but a viscoelasticity. The equivalent modulus of elasticity is directly transferred to viscoelasticity by using the elastic-viscoelastic correspondence principle, which weakens the effect of viscosity. Asphalt mastic behaves more like a viscous material at low frequencies. Therefore, the difference between predicted and measured moduli was larger. With the increase in the loading frequency, asphalt mastic shows more elastically and the predicted modulus was much closer to the measured value.

In order to analyze the effect of the structural asphalt volume fraction on the prediction modulus, the structural asphalt volume fraction c_{sa} was taken from 10% to 60% for

comparative analysis. Due to space limitation, the effect of c_{sa} on the dynamic modulus of MS30 is shown here only; see Figure 8. The modulus of structural asphalt is higher than that of free asphalt, so the predicted modulus increases as the volume fraction of structural asphalt increases. It can be seen that the increase in the volume fraction of structural asphalt is an effective method to increase the dynamic modulus of asphalt mastic through the improvement of the physicochemical effect between fillers and asphalt. From the analysis of Figure 7, the underprediction at low frequencies is caused by the elastic-viscoelastic conversion, which is not related to the structural asphalt volume fraction. When the structural asphalt volume fraction is 40%–50%, the prediction modulus is still lower than the measured value at low frequency. It can be found from Figure 8 that the measured modulus of asphalt mastic is among the predicted values when the volume fraction of structural asphalt is 20%–50%; the volume fraction of structural asphalt of different types of fillers and asphalt will be measured by nano-micro experiments in future research.

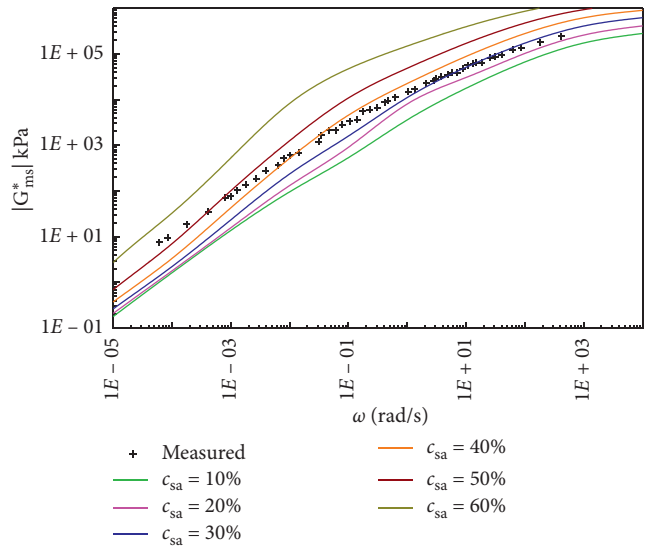

Figure 8: Effect of structural asphalt volume fraction on the prediction modulus of MS30.

5. Parameters Influencing the Dynamic Shear Modulus of Asphalt Mastic

5.1. Effect of Fillers Distribution. The prediction results in Figure 7 were obtained under the assumption that the distribution of fillers is uniform, but the fillers are nonuniformly distributed in the asphalt mastic actually. In order to analyze the influence of fillers distribution on the prediction results of the model, the distribution coefficients are 0.025, 0.05, and 0.25 for comparative analysis. Due to space limitation, the influence of the filler distribution coefficient on the prediction results of MS30 is given here only; see Figure 9.

The decrease in the distribution coefficient means that the particles are dense. From the predicted results in Figure 3, it can be observed that the distribution coefficient decreases and the predicted modulus increases. However, Figure 9 shows an opposite prediction trend. It can be found that the distribution coefficient decreases, and the prediction $|G^*_{ms}|$ decreases. This is due to the use of different prediction models. The prediction results in Figure 3 are obtained by MRP model, and the structural asphalt layer by physicochemical effect is not considered in the model. The distribution coefficient decreases, which results in the decrease of the thickness of the asphalt in the adsorption structure of the fillers considering physicochemical effect. When $\bar{\lambda}/(2R_1) = 0.25$, there is a small amount of accumulation of fillers, and the predicted value slightly decreases. When $\bar{\lambda}/(2R_1) = 0.05$ and 0.025, a large number of agglomerations occur in fillers, and the predicted value decreases obviously. Therefore, in order to improve the viscoelasticity of asphalt mastic, the agglomeration of fillers should be avoided in the actual production process of asphalt mastic.

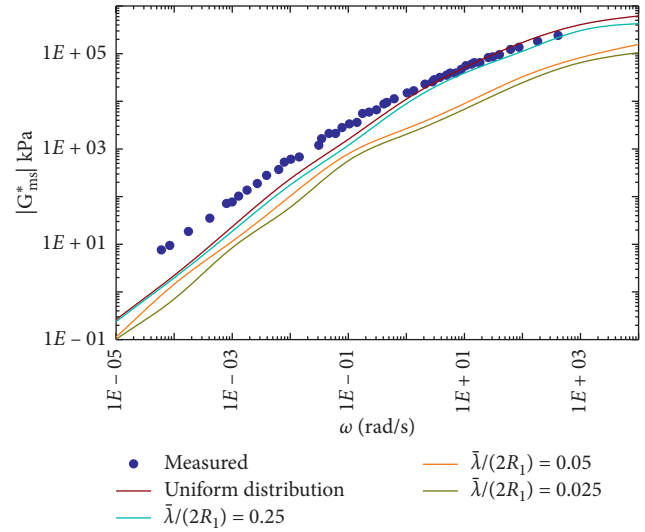

Figure 9: Effect of fillers distribution on the predicted $|G^*_{ms}|$.

5.2. Effect of Fillers Gradation. In order to analyze the influence of the fillers grade on the predicted results of the dynamic shear modulus of asphalt mastic, three different grades of fine, medium, and coarse are used for comparative analysis; see Table 2. Here, only the predicted dynamic shear modulus of the MS30 is shown; see Figure 10.

It can be seen from Figure 10 that the fillers gradation has a considerable influence on the predicted $|G^*_{ms}|$ of MS30, which indicated that the H-MRP model proposed in this study could be well considered for the effect of fillers particle size. Asphalt mastic mixed with fine-grade fillers has the highest predicted modulus; it is due to the fact that the increase of the specific surface area of fillers will enhance the cementation of structural asphalt so that the modulus value increased.

5.3. Effect of Young's Modulus and Poisson's Ratio of Fillers. The influences of Young's modulus E_1 and Poisson's ratio v_1 of fillers on the predicted $|G^*_{ms}|$ of MS30 are shown in Figures 11

Table 2: Different types of fillers gradation.

Mastic types	Sieve opening, mm (%)							
	0.075	0.030	0.023	0.017	0.0077	0.0038	0.0029	0.0013
Coarse	100	50	43	29	14	8	3	0
Medium	100	57	50	36	21	15	10	7
Fine	100	64	57	43	28	22	17	10

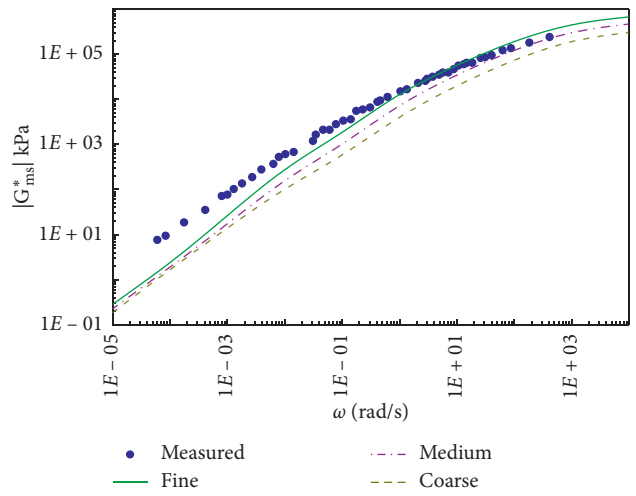

Figure 10: Effect of fillers gradation on predicted $|G^*_{ms}|$.

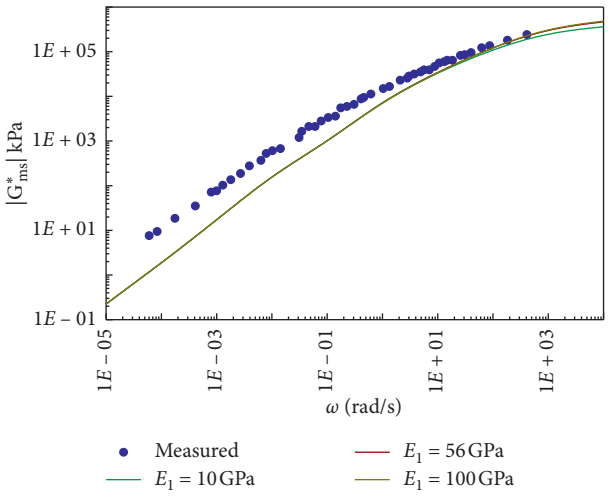

Figure 11: Effect of modulus of fillers on predicted $|G^*_{ms}|$.

and 12. It can be seen that the dynamic modulus of the asphalt mastic increases as the modulus and Poisson's ratio of fillers increase within a certain range; the magnitude of the increase in $|G^*_{ms}|$ is comparably small, which means that the contribution of aggregate to the dynamic modulus improvement of the mixture is limited, given the fixed portion of fillers.

6. Conclusion

(1) A micromechanical prediction model of asphalt mastic was established based on the morphologically representative pattern (MRP) approach. The influences of physicochemical effect between fillers and asphalt, distribution of fillers, and the filler particle size were considered in the model. An explicit solution was derived to predict the dynamic modulus of asphalt mastic.

(2) The DSR test was conducted to verify the prediction effect of the model. When the fillers volume fractions were 10% and 20%, the predicted value was relatively close to the experimental value. When the volume fractions of fillers were 30% and 40%, the predicted value was lower than the measured ones at low frequencies; the reasons for the underprediction were investigated.

(3) The micromechanical model developed in this paper was able to reflect the effect of factors during a parameter influencing analysis. Based on the sensitivity analysis, the use of uniformly distributed fillers and fine fillers was an effective way to increase the dynamic modulus of asphalt mastic.

(4) In the proposed model, the volume fraction of the structural asphalt and the distribution coefficient of the fillers were assumed; the nano-micro test would be conducted to obtain these parameters in the future research to improve the model proposed in this paper.

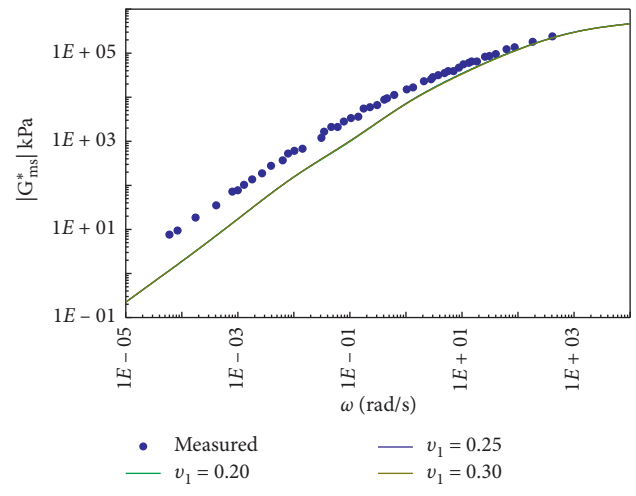

Figure 12: Effect of Poisson's ratio of fillers on predicted $|G^*_{ms}|$.

Data Availability

The data used to support the findings of this study are included within the article.

Conflicts of Interest

The authors declare that there are no conflicts of interest regarding the publication of this paper.

Acknowledgments

This study was funded by the Liaoning Highway Administration Bureau under Grant no. 201701 and National Natural Science Foundation of China under Grant no. 51308084.

References

[1] M. C. Liao, G. Airey, and J. S. Chen, "Mechanical properties of filler-asphalt mastics," *International Journal of Pavement Research & Technology*, vol. 6, no. 5, pp. 576–581, 2013.

[2] J. P. Zhang, J. Z. Pei, and B. G. Wang, "Micromechanical-rheology model for predicting the complex shear modulus of asphalt mastic," *Advanced Materials Research*, vol. 168–170, pp. 523–527, 2010.

[3] G. G. Al-Khateeb, T. S. Khedaywi, and M. F. Irfaeya, "Mechanical behavior of asphalt mastics produced using waste stone sawdust," *Advances in Materials Science and Engineering*, vol. 2018, Article ID 5362397, 10 pages, 2018.

[4] M. W. Witczak and O. A. Fonseca, "Revised predictive model for dynamic (complex) modulus of asphalt mixtures," *Transportation Research Record: Journal of the Transportation Research Board*, vol. 1540, no. 1, pp. 15–23, 1996.

[5] J. Bari and M. W. Witczak, "Development of a new revised version of the Witczak E^* predictive model for hot mix asphalt mixtures," *Journal of the Association of Asphalt Paving Technologists*, vol. 75, pp. 381–423, 2006.

[6] M. Witczak, M. El-Basyouny, and S. El-Badawy, "Incorporation of the new (2005) E^* predictive model in the MEPDG, NCHRP1-40D," Final report, Arizona State University, Tempe, AZ, USA, 2007.

[7] J. Bari and M. Witczak, "New predictive models for viscosity and complex shear modulus of asphalt binders: for use with mechanistic-empirical pavement design guide," *Transportation Research Record Journal of the Transportation Research Board*, vol. 2001, pp. 9–19, 2007.

[8] Z. Hashin, "The elastic moduli of heterogeneous materials," *Journal of Applied Mechanics*, vol. 29, no. 1, pp. 143–150, 1962.

[9] R. Hill, "A self-consistent mechanics of composite materials," *Journal of the Mechanics and Physics of Solids*, vol. 13, no. 4, pp. 213–222, 1965.

[10] R. M. Christensen and K. H. Lo, "Solutions for effective shear properties in three phase sphere and cylinder models," *Journal of the Mechanics and Physics of Solids*, vol. 27, no. 4, pp. 315–330, 1979.

[11] T. Mori and K. Tanaka, "Average stress in matrix and average elastic energy of materials with misfitting inclusions," *Acta Metallurgica*, vol. 21, no. 5, pp. 571–574, 1973.

[12] S.-S. Pang, Y. Li, and J. B. Metcalf, "Elastic modulus prediction of asphalt concrete," *Journal of Materials in Civil Engineering*, vol. 11, no. 3, pp. 236–241, 1999.

[13] R. Luo and R. L. Lytton, "Self-consistent micromechanics models of an asphalt mixture," *Journal of Materials in Civil Engineering*, vol. 23, no. 1, pp. 49–55, 2011.

[14] E. Aigner, R. Lackner, and C. Pichler, "Multiscale prediction of viscoelastic properties of asphalt concrete," *Journal of Materials in Civil Engineering*, vol. 21, no. 12, pp. 771–780, 2009.

[15] X.-y. Zhu, X. Wang, and Y. Yu, "Micromechanical creep models for asphalt-based multi-phase particle-reinforced composites with viscoelastic imperfect interface," *International Journal of Engineering Science*, vol. 76, pp. 34–46, 2014.

[16] X.-Q. Fang and J.-Y. Tian, "Elastic-adhesive interface effect on effective elastic moduli of particulate-reinforced asphalt concrete with large deformation," *International Journal of Engineering Science*, vol. 130, pp. 1–11, 2018.

[17] H. M. Yin, W. G. Buttlar, G. H. Paulino, and H. D. Benedetto, "Assessment of existing micro-mechanical models for asphalt mastics considering viscoelastic effects," *Road Materials and Pavement Design*, vol. 9, no. 1, pp. 31–57, 2008.

[18] B. S. Underwood and Y. R. Kim, "A four phase micro-mechanical model for asphalt mastic modulus," *Mechanics of Materials*, vol. 75, pp. 13–33, 2014.

[19] N. Shashidhar and A. Shenoy, "On using micromechanical models to describe dynamic mechanical behavior of asphalt mastics," *Mechanics of Materials*, vol. 34, no. 10, pp. 657–669, 2002.

[20] W. G. Buttlar and R. Roque, "Evaluation of empirical and theoretical models to determine asphalt mixture stiffnesses at low temperatures," *Asphalt Paving Technology Association of Asphalt Paving Technologists Proceedings of the Technical Sessions*, vol. 65, pp. 99–141, 1996.

[21] B. S. Underwood and Y. R. Kim, "Experimental investigation into the multiscale behaviour of asphalt concrete," *International Journal of Pavement Engineering*, vol. 12, no. 4, pp. 357–370, 2011.

[22] B. Delaporte, H. D. Benedetto, P. Chaverot et al., "Linear viscoelastic properties of bituminous materials: from binders to mastics," *Asphalt Paving Technology Association of Asphalt Paving Technologists Proceedings of the Technical Sessions*, vol. 76, pp. 455–494, 2007.

[23] R. Li, Z. Fan, and P. Wang, "Micromechanics prediction of effective modulus for asphalt mastic considering inter-particle interaction," *Construction and Building Materials*, vol. 101, pp. 209–216, 2015.

[24] C. Davis and C. Castorena, "Implications of physico-chemical interactions in asphalt mastics on asphalt microstructure," *Construction and Building Materials*, vol. 94, pp. 83–89, 2015.

[25] C. Clopotel, R. Velasquez, and H. Bahia, "Measuring physico-chemical interaction in mastics using glass transition," *Road Materials and Pavement Design*, vol. 13, no. 1, pp. 304–320, 2012.

[26] Y. Veytskin, C. Bobko, and C. Castorena, "Nanoindentation and atomic force microscopy investigations of asphalt binder and mastic," *Journal of Materials in Civil Engineering*, vol. 28, no. 6, Article ID 04016019, 2016.

[27] M. Guo, Y. Tan, J. Yu, Y. Hue, and L. Wang, "A direct characterization of interfacial interaction between asphalt binder and mineral fillers by atomic force microscopy," *Materials & Structures*, vol. 50, no. 2, pp. 141.1–141.11, 2017.

[28] V. Marcadon, E. Herve, and A. Zaoui, "Micromechanical modeling of packing and size effects in particulate composites," *International Journal of Solids and Structures*, vol. 44, no. 25-26, pp. 8213–8228, 2007.

[29] M. Majewski, M. Kursa, P. Holobut, and K. Kowalczyk-Gajewska, "Micromechanical and numerical analysis of packing and size effects in elastic particulate composites," *Composites Part B: Engineering*, vol. 124, pp. 158–174, 2017.

[30] E. Herve and A. Zaoui, "inclusion-based micromechanical modelling," *International Journal of Engineering Science*, vol. 31, no. 1, pp. 1–10, 1993.

[31] S. W. Park and R. A. Schapery, "Methods of interconversion between linear viscoelastic material functions. Part I-a numerical method based on Prony series," *International Journal of Solids and Structures*, vol. 36, no. 11, pp. 1653–1675, 1999.

[32] X. Shu and B. Huang, "Dynamic modulus prediction of hma mixtures based on the viscoelastic micromechanical model," *Journal of Materials in Civil Engineering*, vol. 20, no. 8, pp. 530–538, 2008.

[33] H. Di Benedetto, F. Olard, C. Sauzéat, and B. Delaporte, "Linear viscoelastic behaviour of bituminous materials: from binders to mixes," *Road Materials and Pavement Design*, vol. 5, no. 1, pp. 163–202, 2004.